

# One-Time Model Adaptation to Heterogeneous Clients: An Intra-Client and Inter-Image Attention Design

Yikai Yan<sup>1</sup> Chaoyue Niu<sup>1</sup> Fan Wu<sup>1</sup> Qinya Li<sup>1</sup> Shaojie Tang<sup>2</sup> Chengfei Lyu<sup>3</sup>  
Guihai Chen<sup>1</sup>  
<sup>1</sup>Shanghai Jiao Tong University <sup>2</sup>University of Texas at Dallas <sup>3</sup>Alibaba Group

## Abstract

The mainstream workflow of image recognition applications is first training one global model on the cloud for a wide range of classes and then serving numerous clients, each with heterogeneous images from a small subset of classes to be recognized. From the cloud-client discrepancies on the range of image classes, the recognition model is desired to have strong adaptiveness, intuitively by concentrating the focus on each individual client’s local dynamic class subset, while incurring negligible overhead. In this work, we propose to plug a new intra-client and inter-image attention (ICIIA) module into existing backbone recognition models, requiring only one-time cloud-based training to be client-adaptive. In particular, given a target image from a certain client, ICIIA introduces multi-head self-attention to retrieve relevant images from the client’s historical unlabeled images, thereby calibrating the focus and the recognition result. Further considering that ICIIA’s overhead is dominated by linear projection, we propose partitioned linear projection with feature shuffling for replacement and allow increasing the number of partitions to dramatically improve efficiency without scarifying too much accuracy. We finally evaluate ICIIA using 3 different recognition tasks with 9 backbone models over 5 representative datasets. Extensive evaluation results demonstrate the effectiveness and efficiency of ICIIA. Specifically, for ImageNet-1K with the backbone models of MobileNetV3-L and Swin-B, ICIIA can improve the testing accuracy to 83.37% (+8.11%) and 88.86% (+5.28%), while adding only 1.62% and 0.02% of FLOPs, respectively. Source code is available in the supplementary materials.

## 1. Introduction

Nowadays, many vision models have been deployed to recognize client-side images, such as identifying everything with Google Lens, categorizing images in Google Photos, and taking photos to search for products on Amazon Shopping. Let’s examine the workflow of Google Lens, a mobile

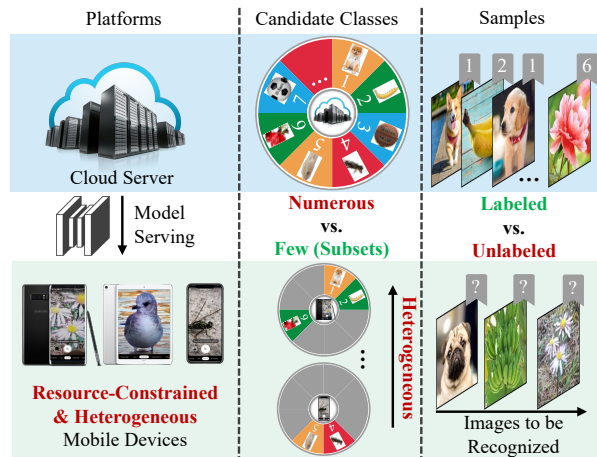


Figure 1. Image recognition from a new cloud-client view.

camera app with strong image recognition capabilities, in detail. A global recognition model is trained on the cloud using a large scale of labeled images, spanning a wide range of classes, including various species of animals and plants, documents, commodities, etc. Then, the recognition model will serve numerous app users once they take photos in daily life, and each user’s photos tend to involve a few classes.

By probing the image recognition scenario from a new cloud-client perspective, we find several important but often neglected characteristics, as illustrated in Fig. 1. (1) The recognition model is optimized for the full set of classes on the cloud, whereas the images to be recognized on each individual client normally come from a small subset of classes. In addition, the class subsets of different clients also differ from each other. Moreover, as a client collects new images over time, the client’s class subset will change dynamically. (2) Different from the cloud with labeled images for training, the images on each client are unlabeled for real-time recognition. It is also practically infeasible to let non-expert users label images and take their annotations as the ground truth. More generally, the missing of labels on the side of clients is an atypical setting of computer vision (CV) scenarios, compared with natural language processing

(NLP) and recommendation applications, which typically predict user interactive behaviors (e.g., next input word, click or browse) and take practical user feedback as labels.

The above cloud-client discrepancies raise the new requirement of strong adaptiveness on the image recognition model, from the cloud’s global full set of classes to each client’s local subset of classes, across different clients’ heterogeneous class subsets, and over a certain client’s dynamic image dataset. Intuitively, the focus of the recognition model was originally distributed on all the classes. When serving a specific client, if the focus can be concentrated on the client’s class subset and further be dynamically adjusted as more unlabeled images are accumulated, the recognition accuracy can be significantly improved.

To achieve model adaptation effectively and efficiently, there still exist several practical challenges. From model architecture, the design should be model-agnostic and lightweight, which is, however, non-trivial. In particular, the design should be compatible with existing backbone networks for image recognition (e.g., convolutional neural network (CNN), transformer, etc.), thereby inheriting their strong representation abilities and being convenient to be implemented and deployed. In addition, no matter whether the recognition model was originally deployed on the cloud to serve a large scale of clients or offloaded to resource-constrained and heterogeneous clients for local serving, the design would better introduce only a small size of parameters and negligible overhead to guarantee high efficiency (e.g., low response latency). Of course, in the resource-rich context, scaling up the design for better accuracy should be an available option. From learning algorithm, although client-specific fine-tuning is model-agnostic and even does not need extra parameters, the missing of labels and the resource constraints of clients make such type of methods inapplicable to image recognition. Therefore, it is highly desirable, yet challenging, to adapt the model only once on the cloud and circumvent on-client retraining.

In this work, we propose an Intra-Client and Inter-Image Attention (ICIIA) module, which is pluggable between the feature extractor and the classifier of an arbitrary backbone model for image recognition. After one-time training on the cloud, ICIIA can well adapt to heterogeneous clients. The key insight behind ICIIA’s strong adaptiveness is that when serving a specific client, given a target image, ICIIA retrieves the relevant images from the client’s historical images and enables the recognition model to concentrate on the local dynamic subset of classes, thereby calibrating the features and the recognition results. In contrast, the conventional mainstream mode is recognizing the images independently, failing to exploit each individual client’s historical unlabeled images. The underlying building block of ICIIA is the celebrated multi-head self-attention mechanism, which was first proposed in NLP [58] and later ex-

tended to computer vision [12], and has achieved the state-of-art performance by capturing the intra-sample dependencies among words or image patches. At a totally different level, ICIIA intends to capture the inter-image dependencies for each individual client. In particular, the attention operation is performed over the separate pool of a certain client’s local images to be recognized. Through naturally inputting the personalized images from the client rather than manually inserting additional client-specific parameters, ICIIA can achieve adaptiveness in a desired one-for-all way. Further, as the client accumulates more unlabeled images for attention, the performance of ICIIA will become better. Another key difference from the conventional multi-head self-attention mechanism is in linear projection, which originally needs a large size of parameters and incurs high overhead. ICIIA partitions the input features into several blocks and linearly projects for each block individually. To mitigate the side effect of isolating features in different partitions, ICIIA further shuffles the features across partitions. Through the partitioned linear projection with feature shuffling, ICIIA reduces the parameter size to the reciprocal of the number of partitions, while incurring only a slight drop in accuracy, compared with the conventional linear projection. By varying the number of partitions, ICIIA can well balance efficiency and accuracy.

We summarize our key contributions as follows:

- From a new cloud-client perspective to view the image recognition application, we find the discrepancies and the variations on the range of candidate classes. We further identify the new requirement of one-time model adaptation to all the heterogeneous clients under the practical setting of unlabeled images.
- We propose a pluggable ICIIA module upon existing backbone image recognition models. To the best of our knowledge, ICIIA is the first to leverage the attention mechanism to mine intra-client and inter-image dependencies, thereby achieving strong model adaptiveness.
- We further propose partitioned linear projection with feature shuffling to deal with the efficiency problem of the attention layer’s conventional linear projection in serving a large scale of resource-constrained clients.
- We extensively evaluate ICIIA, with several baselines for comparison and variants for ablation study. Evaluation results reveal ICIIA’s effective and efficient adaptation to heterogeneous clients, significant improvements over the original backbone models and tuning methods, and the necessity of each ingredient.

## 2. Related Work

**Model adaptation** Adapting the global model trained on the cloud to serve heterogeneous clients is an important

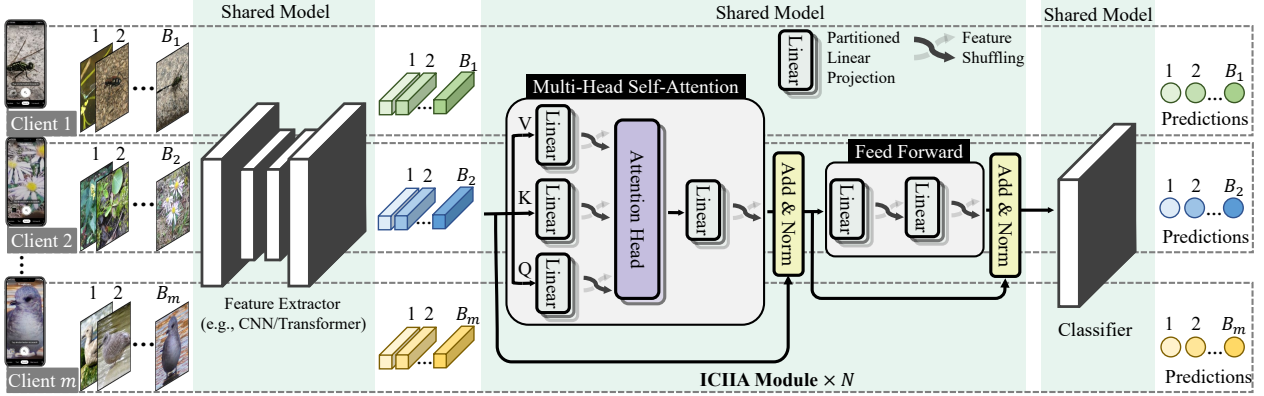


Figure 2. Overall model architecture. The new ICIIA module is plugable between the feature extractor and the classifier of an arbitrary image recognition backbone network for effective and efficient adaptation to heterogeneous clients.

problem in practice. Rather than the cloud-to-client adaptation considered in this work, existing literature mainly considered task-to-task adaptation, either from upstream to downstream [2, 3, 9, 17, 18, 21, 23, 25, 29, 34, 35, 44, 45, 63] (e.g., from masked auto-encoding to classification), from one domain to another [13, 14, 16, 32, 33, 59, 61, 68] (e.g., from natural images to synthesized images or from daytime scenes to nighttime scenes), or across multiple modalities [6, 24, 41, 51, 55] (e.g., natural language and vision). A few recent work [10, 60, 62] considered cloud-to-client adaptation in e-commerce recommendation or next-word prediction with the local samples naturally labeled by each client, which differs from the label missing setting of our image recognition scenario. Among these existing work, one line resorted to fine-tuning the pre-trained model on the labeled data of each target task and elaborated on developing new pre-training techniques to facilitate the subsequent fine-tuning process [2, 9, 17, 24, 51] or designing new fine-tuning algorithms [3, 16, 18, 23, 33, 35, 59, 63]. Other works further proposed to modify the backbone model, by inserting learnable task-specific adapters [21, 32, 44, 45, 55] or providing prompts (i.e., a small number of learnable tokens associated with each task) as additional inputs to the NLP models [29, 34] or recently to the CV models [13, 14, 25, 41, 68]. The latter method was also known as “prompt tuning”. Compared with model adaptation to a few target tasks normally with labeled samples, the cloud-to-client recognition model adaptation studied in this work, however, involves a large number of target clients with only unlabeled images, making previous design inapplicable.

Different from cloud-based model training, an emerging federated learning [47] framework enables heterogeneous clients to jointly train a global model without uploading local data. Much related work also focused on the need of adapting the global model to each client, thereby mitigating data heterogeneity [46]. The designs mainly fall into the pattern of letting each client maintain a person-

alized model with client-specific parameters, by leveraging multi-task learning [53], meta learning [5, 15, 26], hypernetworks [43], knowledge distillation [52, 65, 69], model splitting [36, 42], model pruning [30], or loss function regularization [11, 31]. However, federated learning normally require local training with labeled samples, which are unavailable in the scenario of image recognition.

**Attention mechanism** For NLP and recommendation tasks, each sample is naturally represented by a sequence of words or user behaviors. The attention mechanism has been widely adopted to mine the dependencies within the sequence, such that the model can focus on the related words or behaviors for more accurate prediction [58, 66, 67]. In particular, Vaswani et al. [58] proposed a novel architecture, called transformer, based on multi-head attention with residual connections [19] and layer normalization [1], achieving state-of-the-art performance initially on NLP tasks and later on CV tasks [12, 40]. Motivated by the sequential data format in NLP and recommendation, we regard the images to be recognized on each individual client as a sequence, rather than as separate images like in the mainstream recognition models. We thus introduce the attention mechanism and further deal with the efficiency issue of serving a large number of resource-constraint clients.

### 3. Design and Analysis

#### 3.1. Overall Architecture

As shown in Fig. 2, besides a feature extractor and a classifier in an arbitrary backbone recognition model, all the heterogeneous clients will share the new ICIIA module in our model design. Specifically, for each client, the images to be recognized are first input to the feature extractor. The extracted features are then fed into the ICIIA module. Given a target image, ICIIA essentially mines the intra-client and inter-image dependencies to retrieve the relevant historical images, and calibrates the features to let the classifier fo-

cus on the client’s local data distribution (Sec. 3.2). Such a model architecture design can adapt to each heterogeneous client after one-time training on the cloud and dynamically improves the performance as the client accumulates more unlabeled images for attention. Furthermore, to reduce the overhead, the linear projections in the ICIIA module can be replaced with the proposed partitioned linear projection (Sec. 3.3) with feature shuffling (Sec. 3.4). The overhead analysis regarding the number of parameters and FLOPs is described in Sec. 3.5. Finally, the calibrated features from the ICIIA module are input into the classifier to generate the final recognition result.

### 3.2. Intra-Client and Inter-Image Attention

The ICIIA module consists of a multi-head self-attention layer [58] and a feed-forward network with residual connections and layer normalization. The multi-head self-attention layer takes the features of both the historical images and the target image from a certain client as the query vector (Q), the key vector (K), and the value vector (V), linearly projects each vector to  $H$  representation subspaces, and computes the scaled dot-product attention scores with  $H$  attention heads. Then, the features of the target image are calibrated using the weighted average of the features of the historical images, where the weights take the attention scores. The calibrated features are once again linearly projected and finally fed into the feed-forward network.

### 3.3. Partitioned Linear Projection

The original linear projections in the ICIIA module requires a large size of parameters, which may become the bottleneck of cloud-based model serving for numerous clients in low latency or deploying the model to resource-constrained clients for real-time local serving. To overcome this bottleneck, we propose a partitioned version of the linear projection and allow the number of partitions to be adjusted according to the efficiency requirement. As shown in Fig. 3a, the input features are first partitioned into  $P$  small blocks, and then a linear projection with a small size of parameters will be created for each individual block. Suppose the input feature dimension is  $D$ . As illustrated in Fig. 3b, the original linear projection requires  $H \times D \times D/H = D^2$  parameters in total. In contrast, the new partitioned projection needs only  $P \times (D/P)^2 = D^2/P$  parameters. Therefore, the partitioned projection can reduce the number of parameters by a factor of  $P$ .

### 3.4. Feature Shuffling

Compared with the original linear projection, the new partitioned projection can improve efficiency, but isolates the features in different partitions, as depicted in Fig. 3c, which may hurt model performance. To mitigate side effect, we insert a feature shuffling layer after each projection

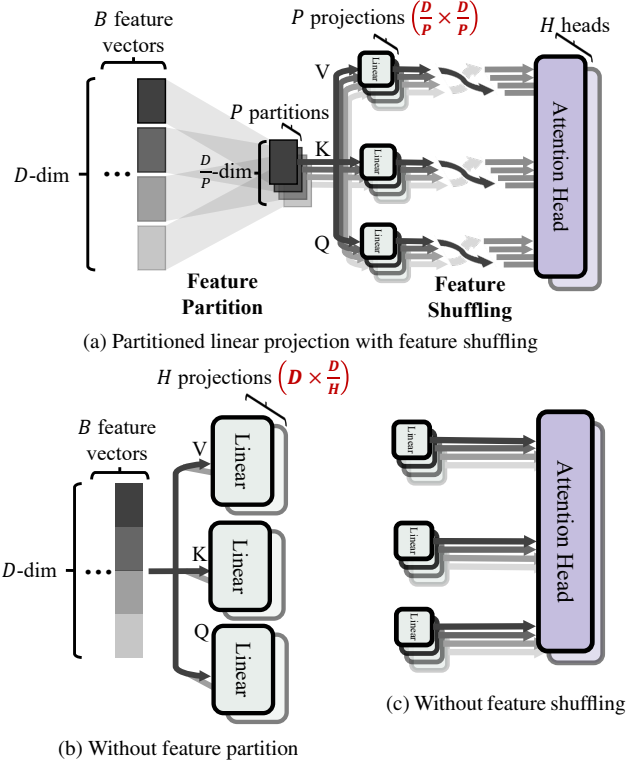


Figure 3. Illustration of the partitioned linear projection and feature shuffling, and comparison with the design without feature partition or without feature shuffling.

layer, mixing the features from different partitions. Such a shuffling layer is implemented using a transpose operation followed by a reshape operation and introduces no additional parameters. By comparing Fig. 3a with Fig. 3c, we can observe that with feature shuffling, each attention head receives features from all the partitions, while without it, each head receives features from only a subset of partitions.

### 3.5. Overhead Analysis

Suppose  $N$  layers of the ICIIA module is adopted, and the attention scores are computed in a window of  $B$  images. Each layer has 6 partitioned linear projections, including 3 input projections for the query, key, and value vectors, 1 output projection, as well as 2 projections in the feed-forward layer, requiring  $6D^2/P$  parameters and  $6BD^2/P$  FLOPs. In addition, the multi-head self-attention operation requires  $B^2D$  FLOPs for computing the attention scores and  $B^2D$  FLOPs for computing the attention outputs. Therefore, the total size of ICIIA-related parameters<sup>1</sup> is  $\#Param. = \frac{6D^2}{P} \times N$ . The ICIIA-related computation overhead<sup>1</sup> for recognizing one target image given  $B - 1$  historical images or recognizing  $B$  images in a batch (e.g.,

<sup>1</sup>The parameters and computation overhead of the residual connections and layer normalization are negligible and thus omitted for conciseness.

	Backbone		ICIIA-B		ICIIA-T	
	#Param.	#FLOPs	#Param.	#FLOPs	#Param.	#FLOPs
MobileNetV3-L [22]	<b>5.5M</b>	<b>0.23G</b>	30M (538%)	0.47G (202%)	0.14M ( <b>2.47%</b> )	3.8M ( <b>1.62%</b> )
ResNet-152 [19]	60M	12G	76M (126%)	1.2G (10.4%)	0.33M ( <b>0.54%</b> )	7.9M ( <b>0.07%</b> )
EfficientNet-B4 [56]	19M	4.6G	58M (299%)	0.93G (20.2%)	0.25M ( <b>1.32%</b> )	6.4M ( <b>0.14%</b> )
Swin-B [37]	88M	15G	19M (21.5%)	0.30G (1.97%)	0.09M ( <b>0.10%</b> )	2.8M ( <b>0.02%</b> )
ConvNeXt-L [39]	198M	34G	43M (21.5%)	0.68G (1.98%)	0.19M ( <b>0.10%</b> )	5.0M ( <b>0.01%</b> )
EfficientNet-B7 [56]	66M	39G	118M (178%)	1.9G (4.86%)	0.50M ( <b>0.76%</b> )	11M ( <b>0.03%</b> )

Table 1. The size of parameters and the number of FLOPs in ICIIA-B and ICIIA-T on *ImageNet-1K* with different backbone models. The percentages in the parentheses denote the relative ratios to the backbone model.

Dataset	Task	#Clients	#Samples	#Classes	Classes per Client	
					mean	stdev
<i>iNaturalist 2019</i> [20]	image classification	2,295	193,210	1,010	45.5	41.8
<i>FEMNIST</i> [4]	image classification	3,597	817,851	62	55.0	6.6
<i>CelebA</i> [38]	multi-label classification	9,343	200,288	N/A	N/A	N/A
<i>ImageNet-1K</i> [8]	image classification	3,161	1,331,167	1,000	15.2	7.1
<i>UCF101</i> [54]	action recognition	121	13,320	101	22.8	9.2

Table 2. The datasets for evaluation, the corresponding recognition tasks, as well as the global and client-level statistics of different datasets.

for the scenario of Google Photos categorizing one client’s many local images) is  $\#FLOPs = \left(\frac{6BD^2}{P} + 2B^2D\right) \times N$ .

To give more intuitions about the practical efficiency of ICIIA, we introduce two different configurations: one is the base version with the conventional linear projections (i.e.,  $P = 1$ ), called ICIIA-B; and the other is the tiny version with  $P = 256$  partitions, called ICIIA-T. We take 6 different backbone image recognition models to be evaluated over *ImageNet-1K*, set the number of ICIIA layers to  $N = 3$ , and set the window size for computing attention scores to  $B = 16$ . Tab. 1 lists the detailed size of parameters and FLOPs in ICIIA-B and ICIIA-T, as well as their relative ratios to those of the backbone. We find that compared with ICIIA-B, ICIIA-T sharply reduces the parameter size and FLOPs via the partitioned linear projection, and meanwhile, introduces quite low overhead compared with the backbone, even for some light-weight networks (e.g., MobileNetV3-L [22]) that can be deployed on mobile devices.

## 4. Evaluation

### 4.1. Setup

**Datasets and recognition tasks** We extensively evaluate ICIIA with 3 different tasks on 5 representative datasets, involving 9 benchmark models.

*iNaturalist 2019* [20] contains images of 1,010 species of plants and animals collected and verified by the users from *iNaturalist*<sup>2</sup>, a citizen science website for naturalists. The

<sup>2</sup>[www.inaturalist.org](http://www.inaturalist.org)

task is to recognize the species of the images. We adopt the natural user partition of FedScale [27], allocating each image to the corresponding user who holds the rights, while splitting the user pool into 1,901 users for training and 394 ones for testing. We leave out 20% of the users originally for training now for validation use. We take EfficientNet-B0 [56] as the recognition model.

*FEMNIST* [4] is a dataset for recognizing hand-written digits and characters, and was built by LEAF [4] through naturally partitioning Extended MNIST [7, 28] based on the writer. LEAF originally takes 90% and 10% of each writer’s samples for on-client training and testing, respectively. We separate out 20% of the training samples for validation. We adopt the CNN architecture officially provided by LEAF.

*CelebA* [38] contains face images of 10,177 celebrities, each with 40 binary attribute annotations. The task is to recognize the attributes. Since the attributes of being “male” or not and being “young” or not are normally unique and easy to be inferred for a certain user’s images, we remove these 2 attributes and keep the other 38 attributes for recognition. We take LEAF’s [4] natural user partition based on face ID, dividing the user pool into 8,408 users for training and 935 ones for testing. We still leave out 20% of the users originally for training now for validation. For multi-label classification, we replace the final layer of EfficientNet-B0 [56] with multiple linear classifiers, one for each attribute.

*ImageNet-1K* [8] contains 1,331,167 images of 1,000 classes organized under the hierarchy of WordNet [49] with 85 parent categories. We take the official train-test split and

perform manual dataset splitting for different users, where each user holds roughly 324, 81, and 16 samples from a specific parent category for training, validation, and testing, respectively. We adopt MobileNetV3-L [22], ResNet-152 [19], EfficientNet-B4 [56], Swin-B [37], ConvNeXt-L [39], and EfficientNet-B7 [56].

*UCF101* [54] contains 13,320 videos of 101 action classes and 5 general/parent action categories. The manual dataset splitting is similar to that for *ImageNet-1K*, where the difference is that each user takes roughly 62, 16, and 32 videos from a certain parent category for training, validation, and testing, respectively. Regarding the action recognition model, we take C3D [57].

We also list some statistics of the datasets in Tab. 2. We can observe that no matter by natural partition or manual partition, each client’s local dataset involves a (normally small) subset of all the classes, validating the starting point of the model adaptiveness requirement.

**Baselines and implementation details** We introduce 3 baselines, including the original backbone model, fine-tuning, and prompt tuning, for comparison.

*Original backbone model* takes the mainstream recognition network architectures without the ICIIA module. In addition, the backbone model is optimized over the global training set (i.e., a mixture of all the clients’ training sets). We initialize EfficientNets, the other models over *ImageNet-1K*, and C3D, by loading the weights pre-trained over *ImageNet-1K* from efficientnet-pytorch [48], torchvision [50], and pytorch-video-recognition [64], respectively. For *iNaturalist 2019*, *CelebA*, and *UCF101*, we further tune the pre-trained models over the global training set. For *FEMNIST*, we train the CNN model from scratch.

*Fine-tuning* is to let each client fine-tune the backbone model over its local training dataset and is a classical method for model adaptation. In the experiment, we fine-tune only the last layer of the backbone model (i.e., the classifier(s)) and freeze the other layers, which can function as a static feature extractor. We note that fine-tuning is not applicable to *iNaturalist 2019* or *CelebA*, because the train-test splits of these two datasets are by users, and the users in the training dataset for fine-tuning do not appear in the testing dataset.

*Prompt tuning*, as introduced in Sec. 2, was an enhanced version of fine-tuning and was originally for NLP. We adapt this method to our context by associating each client with a prompt token and feed it as an extra input to the recognition models. We try and optimally set the dimension of the prompt tokens to half of the feature dimension  $D/2$ .

For the settings of our ICIIA module, we evaluate the two configurations of ICIIA-B and ICIIA-T introduced in Sec. 3.5. We try and take the optimal number of layers for each task (i.e.,  $N = 1$  for *FEMNIST* and *CelebA*,  $N = 2$  for

*iNaturalist 2019* and *UCF101*, and  $N = 3$  for *ImageNet-1K*); and take  $H = 4$  attention heads for all the tasks.

We implement all the models and learning algorithms with PyTorch (torch 1.12.1, torchvision 0.13.1). We use stochastic gradient descent (SGD) as the optimizer. By default, the learning rate is set to 0.01, and the batch size is set to 16. More detailed settings are deferred to Appendix A.

## 4.2. Adaptiveness to Heterogeneous Clients

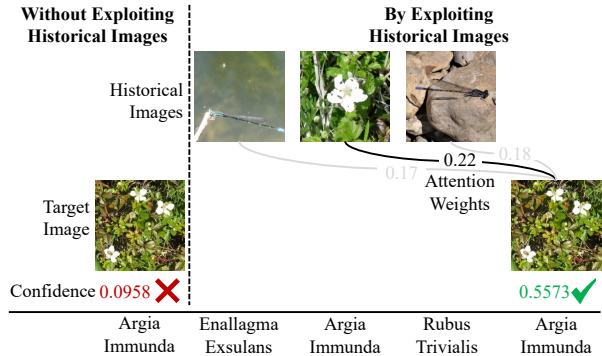


Figure 4. Adaptation to client #1919 in *iNaturalist 2019*.

**Calibration from historical recognized images** We first visualize why ICIIA can adapt to each client’s local data distribution in the recognition phase. We pick client #1919 from *iNaturalist 2019*’s testing set and illustrate how ICIIA-B calibrates the classification from historical images in Fig. 4. We can see that without exploiting any historical image, the original backbone model will misclassify the target image. In contrast, with 3 historical images, ICIIA-B pays the most attention to the second image from the same class (i.e., *argia immunda*) with the target one, improves the confidence on the target class, and classifies correctly.

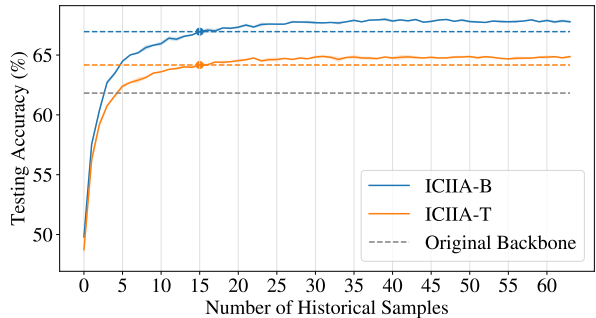


Figure 5. Testing accuracy of ICIIA over *iNaturalist 2019* by varying the number of historical samples. The dashed lines correspond to the training setting of 15 historical samples.

We also plot how the testing accuracy of ICIIA-B and ICIIA-T changes with the accumulation of historical images in Fig. 5. One key observation is that ICIIA-B and ICIIA-T can quickly adapt to each client’s local distribution

and outperform the original backbone model using only 3 and 5 historical images, respectively. If a client has not accumulated enough historical images yet, it can trivially switch to the original backbone model, avoiding cold start. The second key observation is that as the size of historical images increases, ICIIA-B and ICIIA-T achieve better performance. Further considering the attention is performed on the batches of 16 images (15 historical images + 1 target image) in the training phase, while ICIIA-B and ICIIA-T continues to improve after accumulating 15 historical images in the prediction phase, we can derive that ICIIA has a very strong generalization ability.

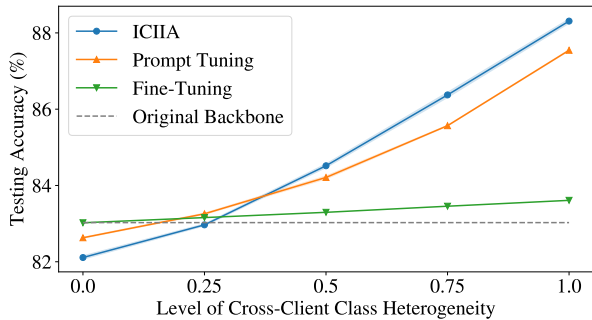
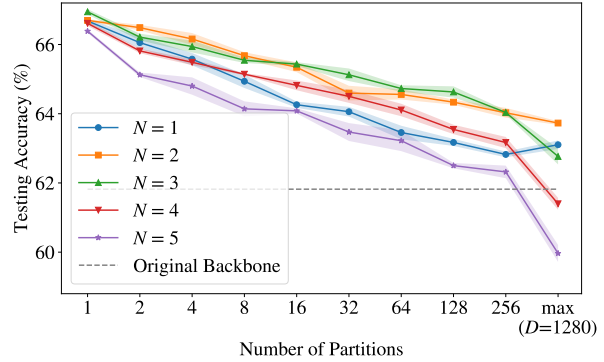


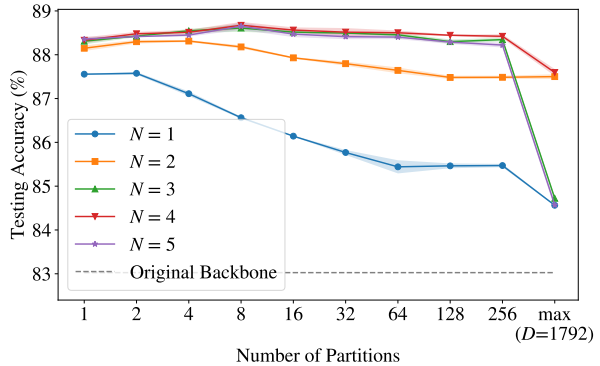
Figure 6. Testing accuracy of ICIIA-B and three baselines over *ImageNet-1K* with EfficientNet-B4, by varying the level of cross-client class heterogeneity, where the level “0” denotes the ideal case of homogeneity.

**Adaptation to cross-client class heterogeneity** We next study how the heterogeneity of the image classes on different clients will affect ICIIA. We use *ImageNet-1K* and vary the client-level dataset splitting. In particular, the first group of clients will now fetch the samples randomly from all the 85 parent categories, while the second group will still fetch from a specific parent category. We view the ratio between the size of the second group and the size of all the clients as a metric of cross-client class heterogeneity. If the ratio is 0, all the clients will fetch samples from all the parent categories, and cross-client class heterogeneity, as well as the cloud-client discrepancy, do not exist. We depict the testing accuracy of ICIIA-B and the three baselines in Fig. 6. We can see that the advantage of ICIIA-B, fine-tuning, and prompt tuning over the original backbone model becomes larger as the level of cross-client class heterogeneity increases, and ICIIA-B performs the best. In the ideal case of no cross-client class heterogeneity, due to the disappearance of the device-cloud discrepancy, all the adaptive methods have no positive effect.

**Adaptation of #partitions  $P$**  We finally evaluate how ICIIA balances model performance and efficiency by taking different numbers of partitions  $P$  in partitioned linear projection. Fig. 7 shows the evaluation results over *iNaturalist 2019* and *ImageNet-1K*, where the number of ICIIA



(a) *iNaturalist 2019* with EfficientNet-B0



(b) *ImageNet-1K* with EfficientNet-B4

Figure 7. Testing accuracy of ICIIA with varying number of partitions  $P$  and layers  $N$ . The “max” on x-axis denotes that  $P$  equals the dimension of the input feature  $D$ . Results are averaged over three repeats, and the shaded region depicts the standard error.

layers  $N$  varies to demonstrate robustness. From Fig. 7, we can see that as  $P$  increases, the parameter size is reduced to  $1/P$  of ICIIA-B’s size, and the testing accuracy of ICIIA will decrease. However, even when  $P$  reaches 256 (i.e., ICIIA-T), the testing accuracy of ICIIA-T is still higher than that of the original backbone model. The advantage and the robustness of ICIIA are more evident over *ImageNet-1K*.

### 4.3. Comparison with Baselines

We compare ICIIA with the baselines and report the testing accuracy in Tab. 3. We can observe consistent and significant improvements of ICIIA over all the baselines on all the datasets and recognition models. (1) By comparing ICIIA-B with the original backbone model, we can draw that ICIIA indeed improves model performance by exploiting each client’s class heterogeneity from the local samples to be recognized; (2) by comparing ICIIA-B with fine-tuning and prompt tuning, we can derive that the intra-client inter-image attention mechanism has the strongest adaptiveness, even without on-client retraining; and (3) by comparing ICIIA-T with ICIIA-B and the baselines, we can draw that although ICIIA-T compromises model accuracy for efficiency, it still significantly outperforms the baselines.

Dataset	Backbone	Original	Fine-Tuning	Prompt Tuning	ICIIA-B	ICIIA-T
<i>iNaturalist 2019</i> [20]	EfficientNet-B0 [56]	61.82%	N/A	N/A	66.70% (+4.88%)	64.03% (+2.21%)
<i>FEMNIST</i> [4]	CNN [4]	88.48%	90.03%	88.47%	91.94% (+3.46%)	91.38% (+2.89%)
<i>CelebA</i> [38]	EfficientNet-B0 [56]	90.84%	N/A	N/A	91.70% (+0.85%)	91.58% (+0.74%)
<i>ImageNet-1K</i> [8]	MobileNetV3-L [22]	75.26%	79.06%	83.93%	84.01% (+8.75%)	83.37% (+8.11%)
	ResNet-152 [19]	82.31%	83.54%	86.85%	88.16% (+5.84%)	87.90% (+5.58%)
	EfficientNet-B4 [56]	83.03%	83.65%	87.54%	88.31% (+5.28%)	88.35% (+5.32%)
	Swin-B [37]	83.58%	84.45%	87.00%	89.23% (+5.65%)	88.86% (+5.28%)
	ConvNeXt-L [39]	84.42%	84.84%	87.59%	89.31% (+4.89%)	89.14% (+4.72%)
	EfficientNet-B7 [56]	84.58%	84.98%	88.71%	89.36% (+4.78%)	89.37% (+4.79%)
<i>UCF101</i> [54]	C3D [57]	79.94%	79.96%	80.01%	81.09% (+1.15%)	80.87% (+0.93%)

Table 3. ICIIA vs. the baselines in terms of testing accuracy. The improvement over the original backbone model is shown in parentheses. The results are averaged over three repeats, each repeat randomly initializing the model parameters excluding the pre-trained weights. The standard errors of the mean are all below 0.24%.

#### 4.4. Ablation Study

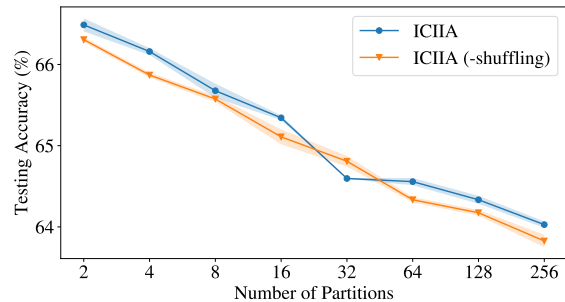
Dataset	ICIIA-B -attention	ICIIA-T -projection	ICIIA-T -shuffling
<i>iNaturalist 2019</i> [20]	-4.78%	-0.30%	-0.20%
<i>ImageNet-1K</i> [8]	-6.50%	-3.62%	-0.28%

Table 4. Drop of testing accuracy after removing different ingredients of ICIIA.

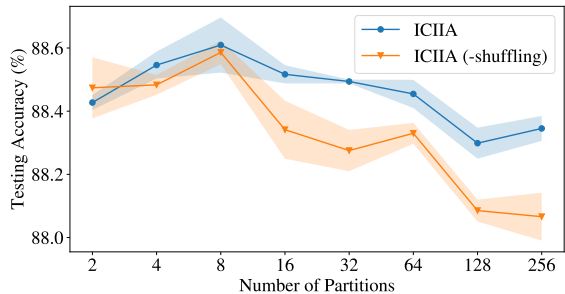
**Impact of intra-client and inter-image attention** We remove the intra-client and inter-image attention operation of ICIIA-B and reserve all the linear projections in both the original multi-head self-attention and feed-forward layers. As shown in the first column of Tab. 4, the testing accuracy sharply drops by 4.78% on *iNaturalist 2019* and by 6.50% on *ImageNet-1K*, which validates the necessity of intra-client and inter-image attention.

**Impact of partitioned linear projection** We remove the partitioned linear projections of ICIIA-T and reserve only the intra-client and inter-image attention operation. From the second column of Tab. 4, we can see that the testing accuracy slightly drops on *iNaturalist 2019*, but dramatically drops by 3.62% on *ImageNet-1K*, validating the necessity of partitioned linear projections.

**Impact of feature shuffling** We remove the feature shuffling operation from ICIIA-T to ablate its impact. We can see from the third column of Tab. 4 that the testing accuracy slightly drops. We also evaluate ICIIA with and without feature shuffling by varying the number of partitions  $P$  in Fig. 8. We can see that the drop of accuracy generally becomes larger for a larger  $P$ . These results validate the necessity of feature shuffling, especially together with a large number of partitioned projections.



(a) *iNaturalist 2019* with EfficientNet-B0



(b) *ImageNet-1K* with EfficientNet-B4

Figure 8. ICIIA with and without feature shuffling, by varying the number of partitions  $P$ .

## 5. Conclusion

In this work, we study the ubiquitous image recognition applications from a new cloud-client perspective. We have proposed a plugable ICIIA module to adapt the backbone recognition model from the cloud’s full set of classes to each individual client’s local dynamic subset of classes, simply after one-time cloud-based training. ICIIA captures intra-client and inter-image dependencies with multi-head self-attention and further improves efficiency by partitioned linear projection along with feature shuffling. We have extensively evaluated ICIIA, revealing effectiveness, efficiency, and superiority.



## References

- [1] Lei Jimmy Ba, Jamie Ryan Kiros, and Geoffrey E. Hinton. Layer normalization. *CoRR*, abs/1607.06450, 2016. 3
- [2] Tom B. Brown, Benjamin Mann, Nick Ryder, Melanie Subbiah, Jared Kaplan, Prafulla Dhariwal, Arvind Neelakantan, Pranav Shyam, Girish Sastry, Amanda Askell, Sandhini Agarwal, Ariel Herbert-Voss, Gretchen Krueger, Tom Henighan, Rewon Child, Aditya Ramesh, Daniel M. Ziegler, Jeffrey Wu, Clemens Winter, Christopher Hesse, Mark Chen, Eric Sigler, Mateusz Litwin, Scott Gray, Benjamin Chess, Jack Clark, Christopher Berner, Sam McCandlish, Alec Radford, Ilya Sutskever, and Dario Amodei. Language models are few-shot learners. In *NeurIPS*, 2020. 3
- [3] Han Cai, Chuang Gan, Ligeng Zhu, and Song Han. Tinytl: Reduce memory, not parameters for efficient on-device learning. In *NeurIPS*, 2020. 3
- [4] Sebastian Caldas, Peter Wu, Tian Li, Jakub Konečný, H. Brendan McMahan, Virginia Smith, and Ameet Talwalkar. LEAF: A benchmark for federated settings. *CoRR*, abs/1812.01097, 2018. 5, 8
- [5] Fei Chen, Mi Luo, Zhenhua Dong, Zhenguo Li, and Xiquiang He. Federated meta-learning with fast convergence and efficient communication. *CoRR*, abs/1802.07876, 2018. 3
- [6] Jun Chen, Han Guo, Kai Yi, Boyang Li, and Mohamed Elhoseiny. Visualgpt: Data-efficient adaptation of pretrained language models for image captioning. In *CVPR*, 2022. 3
- [7] Gregory Cohen, Saeed Afshar, Jonathan Tapson, and André van Schaik. EMNIST: an extension of MNIST to handwritten letters. *CoRR*, abs/1702.05373, 2017. 5
- [8] Jia Deng, Wei Dong, Richard Socher, Li-Jia Li, Kai Li, and Li Fei-Fei. Imagenet: A large-scale hierarchical image database. In *CVPR*, 2009. 5, 8
- [9] Jacob Devlin, Ming-Wei Chang, Kenton Lee, and Kristina Toutanova. BERT: pre-training of deep bidirectional transformers for language understanding. In *NAACL-HLT (1)*, 2019. 3
- [10] Yucheng Ding, Chaoyue Niu, Fan Wu, Shaojie Tang, Chengfei Lyu, and Guihai Chen. On-device model fine-tuning with label correction in recommender systems. *CoRR*, abs/2211.01163, 2022. 3
- [11] Canh T. Dinh, Nguyen Hoang Tran, and Tuan Dung Nguyen. Personalized federated learning with moreau envelopes. In *NeurIPS*, 2020. 3
- [12] Alexey Dosovitskiy, Lucas Beyer, Alexander Kolesnikov, Dirk Weissenborn, Xiaohua Zhai, Thomas Unterthiner, Mostafa Dehghani, Matthias Minderer, Georg Heigold, Sylvain Gelly, Jakob Uszkoreit, and Neil Houlsby. An image is worth 16x16 words: Transformers for image recognition at scale. In *ICLR*, 2021. 2, 3
- [13] Yu Du, Fangyun Wei, Zihe Zhang, Miaojing Shi, Yue Gao, and Guoqi Li. Learning to prompt for open-vocabulary object detection with vision-language model. In *CVPR*, 2022. 3
- [14] Yu Du, Fangyun Wei, Zihe Zhang, Miaojing Shi, Yue Gao, and Guoqi Li. Learning to prompt for open-vocabulary object detection with vision-language model. In *CVPR*, 2022. 3
- [15] Alireza Fallah, Aryan Mokhtari, and Asuman E. Ozdaglar. Personalized federated learning with theoretical guarantees: A model-agnostic meta-learning approach. In *NeurIPS*, 2020. 3
- [16] Yunhui Guo, Honghui Shi, Abhishek Kumar, Kristen Grauman, Tajana Rosing, and Rogério Schmidt Feris. Spottune: Transfer learning through adaptive fine-tuning. In *CVPR*, 2019. 3
- [17] Kaiming He, Xinlei Chen, Saining Xie, Yanghao Li, Piotr Dollár, and Ross B. Girshick. Masked autoencoders are scalable vision learners. In *CVPR*, 2022. 3
- [18] Kaiming He, Haoqi Fan, Yuxin Wu, Saining Xie, and Ross B. Girshick. Momentum contrast for unsupervised visual representation learning. In *CVPR*, 2020. 3
- [19] Kaiming He, Xiangyu Zhang, Shaoqing Ren, and Jian Sun. Deep residual learning for image recognition. In *CVPR*, 2016. 3, 5, 6, 8
- [20] Grant Van Horn and Oisín Mac Aodha. iNaturalist 2019. <https://sites.google.com/view/fgvc6/competitions/inaturalist-2019>, 2019. 5, 8
- [21] Neil Houlsby, Andrei Giurgiu, Stanislaw Jastrzebski, Bruna Morrone, Quentin de Laroussilhe, Andrea Gesmundo, Mona Attariyan, and Sylvain Gelly. Parameter-efficient transfer learning for NLP. In *ICML*, 2019. 3
- [22] Andrew Howard, Ruoming Pang, Hartwig Adam, Quoc V. Le, Mark Sandler, Bo Chen, Weijun Wang, Liang-Chieh Chen, Mingxing Tan, Grace Chu, Vijay Vasudevan, and Yukun Zhu. Searching for mobilenetv3. In *ICCV*, 2019. 5, 6, 8
- [23] Edward J. Hu, Yelong Shen, Phillip Wallis, Zeyuan Allen-Zhu, Yuanzhi Li, Shean Wang, Lu Wang, and Weizhu Chen. Lora: Low-rank adaptation of large language models. In *ICLR*, 2022. 3
- [24] Chao Jia, Yinfei Yang, Ye Xia, Yi-Ting Chen, Zarana Parekh, Hieu Pham, Quoc V. Le, Yun-Hsuan Sung, Zhen Li, and Tom Duerig. Scaling up visual and vision-language representation learning with noisy text supervision. In *ICML*, 2021. 3
- [25] Menglin Jia, Luming Tang, Bor-Chun Chen, Claire Cardie, Serge J. Belongie, Bharath Hariharan, and Ser-Nam Lim. Visual prompt tuning. In *ECCV (33)*, 2022. 3
- [26] Yihan Jiang, Jakub Konečný, Keith Rush, and Sreeram Kannan. Improving federated learning personalization via model agnostic meta learning. *CoRR*, abs/1909.12488, 2019. 3
- [27] Fan Lai, Yinwei Dai, Sanjay Sri Vallabh Singapuram, Jiaachen Liu, Xiangfeng Zhu, Harsha V. Madhyastha, and Mosharaf Chowdhury. FedScale: Benchmarking model and system performance of federated learning at scale. In *ICML*, 2022. 5
- [28] Yann LeCun, Léon Bottou, Yoshua Bengio, and Patrick Haffner. Gradient-based learning applied to document recognition. *Proceedings of the IEEE*, 86(11):2278–2324, 1998. 5
- [29] Brian Lester, Rami Al-Rfou, and Noah Constant. The power of scale for parameter-efficient prompt tuning. In *EMNLP (1)*, 2021. 3

- [30] Ang Li, Jingwei Sun, Binghui Wang, Lin Duan, Sicheng Li, Yiran Chen, and Hai Li. Lotteryfl: Personalized and communication-efficient federated learning with lottery ticket hypothesis on non-iid datasets. *CoRR*, abs/2008.03371, 2020. 3
- [31] Tian Li, Shengyuan Hu, Ahmad Beirami, and Virginia Smith. Ditto: Fair and robust federated learning through personalization. In *ICML*, 2021. 3
- [32] Wei-Hong Li, Xialei Liu, and Hakan Bilen. Cross-domain few-shot learning with task-specific adapters. In *CVPR*, 2022. 3
- [33] Xuhong Li, Yves Grandvalet, and Franck Davoine. Explicit inductive bias for transfer learning with convolutional networks. In *ICML*, 2018. 3
- [34] Xiang Lisa Li and Percy Liang. Prefix-tuning: Optimizing continuous prompts for generation. In *ACL/IJCNLP (1)*, 2021. 3
- [35] Dongze Lian, Daquan Zhou, Jiashi Feng, and Xinchao Wang. Scaling & shifting your features: A new baseline for efficient model tuning. *CoRR*, abs/2210.08823, 2022. 3
- [36] Paul Pu Liang, Terrance Liu, Ziyin Liu, Ruslan Salakhutdinov, and Louis-Philippe Morency. Think locally, act globally: Federated learning with local and global representations. *CoRR*, abs/2001.01523, 2020. 3
- [37] Ze Liu, Yutong Lin, Yue Cao, Han Hu, Yixuan Wei, Zheng Zhang, Stephen Lin, and Baining Guo. Swin transformer: Hierarchical vision transformer using shifted windows. In *ICCV*, 2021. 5, 6, 8
- [38] Ziwei Liu, Ping Luo, Xiaogang Wang, and Xiaoou Tang. Deep learning face attributes in the wild. In *ICCV*, 2015. 5, 8
- [39] Zhuang Liu, Hanzi Mao, Chao-Yuan Wu, Christoph Feichtenhofer, Trevor Darrell, and Saining Xie. A convnet for the 2020s. In *CVPR*, 2022. 5, 6, 8
- [40] Ze Liu, Jia Ning, Yue Cao, Yixuan Wei, Zheng Zhang, Stephen Lin, and Han Hu. Video swin transformer. In *CVPR*, 2022. 3
- [41] Yuning Lu, Jianzhuang Liu, Yonggang Zhang, Yajing Liu, and Xinmei Tian. Prompt distribution learning. In *CVPR*, 2022. 3
- [42] Mi Luo, Fei Chen, Dapeng Hu, Yifan Zhang, Jian Liang, and Jiashi Feng. No fear of heterogeneity: Classifier calibration for federated learning with non-iid data. In *NeurIPS*, 2021. 3
- [43] Xiaosong Ma, Jie Zhang, Song Guo, and Wenchao Xu. Layer-wised model aggregation for personalized federated learning. In *CVPR*, 2022. 3
- [44] Rabeeh Karimi Mahabadi, James Henderson, and Sebastian Ruder. Compacter: Efficient low-rank hypercomplex adapter layers. In *NeurIPS*, 2021. 3
- [45] Rabeeh Karimi Mahabadi, Sebastian Ruder, Mostafa Dehghani, and James Henderson. Parameter-efficient multi-task fine-tuning for transformers via shared hypernetworks. In *ACL/IJCNLP (1)*, 2021. 3
- [46] Yishay Mansour, Mehryar Mohri, Jae Ro, and Ananda Theertha Suresh. Three approaches for personalization with applications to federated learning. *CoRR*, abs/2002.10619, 2020. 3
- [47] Brendan McMahan, Eider Moore, Daniel Ramage, Seth Hampson, and Blaise Agüera y Arcas. Communication-efficient learning of deep networks from decentralized data. In *AISTATS*, 2017. 3
- [48] Luke Melas-Kyriazi. EfficientNet-PyTorch. <https://github.com/lukemelas/EfficientNet-PyTorch>, 2021. 6
- [49] George A. Miller. Wordnet: A lexical database for english. *Communications of the ACM*, 38(11):39–41, 1995. 5
- [50] Adam Paszke, Sam Gross, Francisco Massa, Adam Lerer, James Bradbury, Gregory Chanan, Trevor Killeen, Zeming Lin, Natalia Gimelshein, Luca Antiga, Alban Desmaison, Andreas Köpf, Edward Z. Yang, Zachary DeVito, Martin Raison, Alykhan Tejani, Sasank Chilamkurthy, Benoit Steiner, Lu Fang, Junjie Bai, and Soumith Chintala. Pytorch: An imperative style, high-performance deep learning library. In *NeurIPS*, 2019. 6
- [51] Alec Radford, Jong Wook Kim, Chris Hallacy, Aditya Ramesh, Gabriel Goh, Sandhini Agarwal, Girish Sastry, Amanda Askell, Pamela Mishkin, Jack Clark, Gretchen Krueger, and Ilya Sutskever. Learning transferable visual models from natural language supervision. In *ICML*, 2021. 3
- [52] Yiqing Shen, Yuyin Zhou, and Lequan Yu. Cd<sup>2</sup>-pfed: Cyclic distillation-guided channel decoupling for model personalization in federated learning. In *CVPR*, 2022. 3
- [53] Virginia Smith, Chao-Kai Chiang, Maziar Sanjabi, and Ameeet Talwalkar. Federated multi-task learning. In *NeurIPS*, 2017. 3
- [54] Khurram Soomro, Amir Roshan Zamir, and Mubarak Shah. UCF101: A dataset of 101 human actions classes from videos in the wild. *CoRR*, abs/1212.0402, 2012. 5, 6, 8
- [55] Yi-Lin Sung, Jaemin Cho, and Mohit Bansal. VL-ADAPTER: parameter-efficient transfer learning for vision-and-language tasks. In *CVPR*, 2022. 3
- [56] Mingxing Tan and Quoc V. Le. Efficientnet: Rethinking model scaling for convolutional neural networks. In *ICML*, 2019. 5, 6, 8
- [57] Du Tran, Lubomir D. Bourdev, Rob Fergus, Lorenzo Torresani, and Manohar Paluri. Learning spatiotemporal features with 3d convolutional networks. In *ICCV*, 2015. 6, 8
- [58] Ashish Vaswani, Noam Shazeer, Niki Parmar, Jakob Uszkoreit, Llion Jones, Aidan N. Gomez, Lukasz Kaiser, and Illia Polosukhin. Attention is all you need. In *NeurIPS*, 2017. 2, 3, 4
- [59] Fan Wang, Zhongyi Han, Yongshun Gong, and Yilong Yin. Exploring domain-invariant parameters for source free domain adaptation. In *CVPR*, 2022. 3
- [60] Yikai Yan, Chaoyue Niu, Renjie Gu, Fan Wu, Shaojie Tang, Lifeng Hua, Chengfei Lyu, and Guihai Chen. On-device learning for model personalization with large-scale cloud-coordinated domain adaptation. In *KDD*, 2022. 3
- [61] Junjie Ye, Changhong Fu, Guangze Zheng, Danda Pani Paudel, and Guang Chen. Unsupervised domain adaptation for nighttime aerial tracking. In *CVPR*, 2022. 3
- [62] Runsheng Yu, Yu Gong, Xu He, Yu Zhu, Qingwen Liu, Wenwu Ou, and Bo An. Personalized adaptive meta learning for cold-start user preference prediction. In *AAAI*, 2021. 3

- [63] Elad Ben Zaken, Yoav Goldberg, and Shauli Ravfogel. Bitfit: Simple parameter-efficient fine-tuning for transformer-based masked language-models. In *ACL (2)*, 2022. 3
- [64] Jianfeng Zhang. Pytorch-Video-Recognition. <https://github.com/jfzhang95/pytorch-video-recognition>, 2019. 6
- [65] Lin Zhang, Li Shen, Liang Ding, Dacheng Tao, and Ling-Yu Duan. Fine-tuning global model via data-free knowledge distillation for non-iid federated learning. In *CVPR*, 2022. 3
- [66] Guorui Zhou, Na Mou, Ying Fan, Qi Pi, Weijie Bian, Chang Zhou, Xiaoqiang Zhu, and Kun Gai. Deep interest evolution network for click-through rate prediction. In *AAAI*, 2019. 3
- [67] Guorui Zhou, Xiaoqiang Zhu, Chengru Song, Ying Fan, Han Zhu, Xiao Ma, Yanghui Yan, Junqi Jin, Han Li, and Kun Gai. Deep interest network for click-through rate prediction. In *KDD*, 2018. 3
- [68] Kaiyang Zhou, Jingkang Yang, Chen Change Loy, and Ziwei Liu. Learning to prompt for vision-language models. *International Journal of Computer Vision*, 130(9):2337–2348, 2022. 3
- [69] Zhuangdi Zhu, Junyuan Hong, and Jiayu Zhou. Data-free knowledge distillation for heterogeneous federated learning. In *ICML*, 2021. 3

## A. Supplementary Notes on the Evaluation

For pretraining the original backbone model, we consistently set the batch size to 32 and the weight decay to 0.0005. Regarding the learning rate, we have tried different recipes and chosen the one which achieves the highest accuracy on the validation set for each dataset:

***iNaturalist 2019*** We use a momentum factor of 0.9 and set the initial learning rate to 0.01 for the last layer and 0.001 for the other layers, and let it decay by 0.1 every 10 epochs.

***CelebA*** We set a constant learning rate of 0.01 with a momentum factor of 0.9.

***FEMNIST and UCF101*** We set a constant learning rate of 0.01 without momentum.

For the proposed ICIIA and the two baselines of fine-tuning and prompt tuning, we consistently set the batch size to 16, which is the best choice among 2, 4, 8, 16, and 32, and set the learning rate to a constant value of 0.01. A special case is *CelebA*, where the number of samples per client is small, often below the default value of 16, and we make each client one batch. Regarding the number of attention heads  $H$  in ICIIA, we have tried the values of 1, 2, 4 and 8, and choose  $H = 4$  which achieves the highest accuracy on the validation dataset. For the dimension of the prompt tokens in prompt tuning, we have tried,  $D/4$ ,  $D/2$ ,  $D$ ,  $2D$  and  $4D$ , and choose  $D/2$  which achieves the highest accuracy on the validation dataset.

We conduct evaluation on machines with operating system Ubuntu 18.04.3, CUDA version 11.4, python version 3.7.13, and two NVIDIA GeForce RTX 2080Ti GPUs. For each run, we train the model for at most 100 epochs, stop early if the accuracy on the validation dataset has not improved for 10 epochs, and adopt the model with the highest accuracy on the validation dataset. Each run takes roughly ten hours to complete. For each result that requires random weight initialization, we repeat with three random seeds and report the average accuracy on the testing dataset.

Source code and the detailed instructions to reproduce the results are available in our supplementary materials.